Virology 446 (2013) 37–48

Contents lists available at ScienceDirect

Virology

journal homepage: www.elsevier.com/locate/yviro

Distinct host cell fates for human malignant melanoma targeted by oncolytic rodent parvoviruses

Ellen M. Vollmers [a,c], Peter Tattersall [b,c,*]

[a] Medical Scientist Training Program, Yale University Medical School, 333 Cedar Street, New Haven, CT 06510, United States
[b] Department of Laboratory Medicine, Yale University Medical School, 333 Cedar Street, New Haven, CT 06510, United States
[c] Department of Genetics, Yale University Medical School, 333 Cedar Street, New Haven, CT 06510, United States

ARTICLE INFO

Available online 9 August 2013

Keywords:
Oncolytic parvovirus
Melanoma
Virus-induced cell death

ABSTRACT

The rodent parvoviruses are known to be oncoselective, and lytically infect many transformed human cells. Because current therapeutic regimens for metastatic melanoma have low response rates and have little effect on improving survival, this disease is a prime candidate for novel approaches to therapy, including oncolytic parvoviruses. Screening of low-passage, patient-derived melanoma cell lines for multiplicity-dependent killing by a panel of five rodent parvoviruses identified LuIII as the most melanoma-lytic. This property was mapped to the LuIII capsid gene, and an efficiently melanoma tropic chimeric virus shown to undergo three types of interaction with primary human melanoma cells: (1) complete lysis of cultures infected at very low multiplicities; (2) acute killing resulting from viral protein synthesis and DNA replication, without concomitant expansion of the infection, due to failure to export progeny virions efficiently; or (3) complete resistance that operates at an intracellular step following virion uptake, but preceding viral transcription.

Introduction

Malignant melanoma is a devastating, aggressive form of skin cancer, derived from melanocytes, the pigment-producing cells in the skin. It is responsible for roughly 75% of skin cancer deaths, despite being one of the rarest forms of skin cancer, and its incidence has been on the rise for the past 30 years (Chin et al., 2006). Life expectancy at diagnosis is fewer than 12 months with current therapies offering little improvements to long-term survival (Hocker et al., 2008). Dacarbazine, an alkylating agent, has been the standard treatment for melanoma since the 1970s (Wolchok, 2012). In 2010, the addition of the immune-modulating anti-CTLA4 monoclonal antibody ipilimumab extended overall survival from 9 to 11 months following diagnosis (Robert et al., 2011). More recently, the FDA approved vemurafenib, a small molecule BRAF kinase inhibitor, specifically for patients bearing the V600E mutation of BRAF (present in 40–60% of spontaneous cases). In this population, the drug increases median survival to 15 months (Ravnan and Matalka, 2012). The limited efficacy of these cutting-edge treatments indicates that this malignancy represents a prime candidate for novel approaches to therapy.

Some viruses possess the unique ability to target and destroy cancer cells while having little to no effect on the untransformed parent tissue (Donahue et al., 2002). Therapy with such "oncolytic viruses" offers additional desirable features, such as the ability to locally amplify their dose at the site of the tumor and to provoke an immune response to antigens expressed by dying tumor cells, all while leaving healthy tissues unharmed (Prestwich et al., 2008). Rodent parvoviruses are inherently oncoselective and oncolytic in many human tumor cell lines, and importantly have the added advantage of being non-pathogenic in humans (Dupont, 2003). Autonomously replicating parvoviruses belonging to the genus *Parvovirus*, such as Minute Virus of Mice, MVM, are small, single-stranded DNA viruses with a linear genome ~5 kb in length (Tijssen et al., 2011). Following binding to a currently uncharacterized receptor, and uptake via receptor-mediated endocytosis, the MVM virion traffics to the nucleus, where a host cell DNA polymerase, most likely pol δ, converts the single-stranded genome into a double-stranded form that is active as a transcription template (Cotmore and Tattersall, 2007). Host replicative DNA polymerases, however, are only expressed during the S-phase of the cell cycle, making parvoviruses naturally S-phase dependent, and transcriptionally active only in dividing cells. The completed template contains two promoters, P4 and P38. The initiating P4 promoter drives the expression of two non-structural proteins, NS1 and NS2. NS1 has a variety of functions in the virus lifecycle, including regulation of gene expression, DNA replication and packaging, and induction of cell death (Cotmore and Tattersall, 2013). The function of NS2 is less well understood, though, for MVM, it is required in murine cell infection for efficient DNA replication and capsid assembly. However, NS2 expression is expendable in transformed

* Corresponding author at: Department of Laboratory Medicine, Yale University Medical School, 333 Cedar Street, New Haven, CT 06510, United States.
Fax: +1 203 688 7340.
E-mail address: peter.tattersall@yale.edu (P. Tattersall).

0042-6822/$ - see front matter © 2013 Elsevier Inc. All rights reserved.
http://dx.doi.org/10.1016/j.virol.2013.07.013

human cells, except for its role in early export of progeny virions out of the host cell (Choi et al., 2005; Cotmore et al., 1997; Eichwald et al., 2002; Miller and Pintel, 2002; Naeger et al., 1993). NS1 also transactivates the P38 promoter, which drives expression of the two capsid genes, VP1 and VP2. These proteins assemble in a ~1:5 ratio to form empty capsids, which then package a single of copy of the viral genome, before being released from the cell by an active process prior to cell death, or as a result of cell lysis (Maroto et al., 2004). Previous studies mapping tropism to viral genes demonstrated that the capsid protein plays a major role in determining host range. Two strains of the same parvovirus serotype, MVMp and MVMi, infect a distinct set of host cells, and each is restricted in the other virus′ target cell. However, the lymphotropic MVMi strain can acquire wild type levels of infection in normally restrictive fibroblasts with only two amino acid changes in the capsid protein (Cotmore and Tattersall, 2007). Further, the capsid appears to determine cell tropism not at the level of binding to a target cells, but at a post-entry step (Paglino and Tattersall, 2011).

While much effort has gone towards determining the viral component of host tissue tropism, less effort has been expended on exploring the differences in susceptibility to a single parvovirus serotype of human tumors of the same tissue type. Parvoviruses and parvoviral vectors have been shown to target a variety of human tumor types, demonstrating increased fitness and cytotoxicity in transformed cells as compared to their normal counterparts (Cornelis et al., 1990; Dupont et al., 2000). Glioma, another aggressive and invariably fatal malignancy has been a target of extensive study, including parvovirus infection of rodent models, established human tumor lines, as well as low-passage patient samples (Wollmann et al., 2012). Furthermore, a Phase I clinical trial of H1 parvovirus therapy of glioblastoma multiforme is currently underway in Germany (Geletneky et al., 2010). To date, the study of parvovirus oncolysis of melanoma has been conducted with transplantable mouse models (El Bakkouri et al., 2005; Lang et al., 2006; Raykov et al., 2005; Wetzel et al., 2007), and long-established human melanoma cell lines (Dupont et al., 2000). However, no comprehensive survey of a broad range of rodent parvovirus serotypes against freshly isolated human melanoma cells has been undertaken to date. In the current study we screened a panel of seven antigenically distinct rodent parvoviruses to identify the best candidate virus for targeting malignant melanoma, and further characterized the ability of the leading candidate virus to infect and kill a broad range of low-passage, patient-derived melanoma cell lines.

Results

A subgroup of rodent parvoviruses can kill stepwise-transformed human melanocytes

To identify the most potent oncolytic parvovirus for malignant melanoma, we initially screened a panel of seven antigenically distinct rodent parvovirus serotypes for the ability to kill two stepwise-transformed melanocyte lines. The viruses screened include the murine viruses Minute Virus of Mice (MVMp, the prototype strain) and mouse parvovirus (MPV1), the rat parvoviruses H1, H3 (also known as Kilham Rat Virus), and rat parvovirus (RPV1), and two serotypes of unknown hosts originally isolated from human tumor samples, LuIII and TVX (Fig. 1A) (Hallauer et al., 1972). Stepwise-transformed models were chosen for the initial screen because they contain a minimal number of genetic mutations needed for transformation, and therefore do not also exhibit the numerous collateral mutations that frequently occur as a result of genetic instability in spontaneous tumors, but contribute no advantage to fitness (Chin et al., 2012). Such minimally mutated models should generalize for parvovirus infection across many spontaneous clinical melanomas,

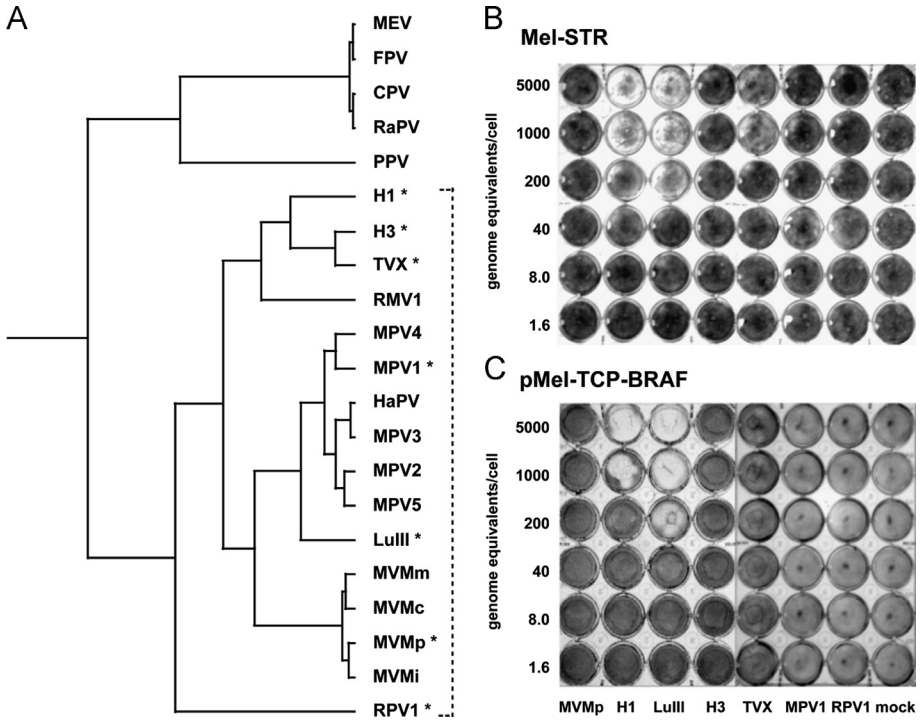

Fig. 1. Identification of the most potent parvovirus for infection and killing of stepwise-transformed melanoma models. Panel A: the phylogenetic tree of the genus *Parvovirus*, based on the protein sequences of the viral coat protein, VP2, and was kindly provided by Susan Cotmore, Derek Gatherer and Andrew Davison. Sequences were aligned using a modification of the Needleman–Wunsch local alignment method as implemented in MOE-Align (http://www.chemcomp.com), and calculated using Bayesian inference with a Yule model of speciation and an exponential relaxed molecular clock. The melanoma killing screens were performed with the seven antigenically distinct parvoviruses, indicated by the asterisks, that cluster within the rodent virus subgroup (dashed bracket). Serial 5-fold dilutions, from 5000 vge/cell, were made of each virus, and added to sub-confluent Mel-STR cells (panel B) or pMel-TCP-BRAF cells (panel C), as described in the Methods section. At 6 days post-infection wells were stained for live cells. Clear and partially clear wells indicate infection and killing of the melanoma cells by the indicated virus.

as spurious outcomes attributable to the unique passenger mutations of any one clinical sample should be avoided. Mel-STR cells (Gupta et al., 2005) have been immortalized with the catalytic subunit of telomerase, then transformed with the SV40 viral oncogenes large T antigen (inactivation of p53 and Rb-family proteins) and small t antigen (PP2A modulation), plus oncogenic RAS (Ras ^{G12V}). Due to the fact that the SV40 T antigens are themselves multifunctional viral replication proteins with oncogenic properties, we were concerned that they might also provide parvovirus helper functions beyond those necessary for cellular transformation. Therefore, we also tested a second stepwise-transformed cell line, pMel-TCP-BRAF (Garraway et al., 2005). This model is transformed without viral oncogenes, instead employing telomerase, constitutively active CDK4 (CDK4^{R24C}), a dominant negative form of p53, and activated BRAF (BRAF^{V600E}). The V600E mutation of BRAF mirrors the human disease, as this point mutation is found in about 60% of clinical melanomas (Davies et al., 2002). To compare the oncolytic potency of each member of the panel of viruses, we performed a multi-well killing assay, in which rapidly dividing target cells were infected with a series of 5-fold dilutions of each of the seven virus serotypes, beginning at an MOI of 5000 vge/cell. Each virus was allowed to infect, kill, and spread through the melanoma culture over 6 days, before staining the remaining live cells (Fig. 1B and C). Five of the seven parvovirus, MVM, H3, TVX, MPV, and RPV, displayed no killing in either of the two stepwise-transformed melanoma models, even at the highest MOI used. However, both tumor models were productively infected by the parvoviruses H1 and LuIII, as demonstrated by wells fully or partially cleared of live melanoma cells. In both cases, H1 efficiently kills the culture from an input of 1000 vge/cell, and shows evidence of killing at the 200 vge/cell dilution demonstrated by incomplete growth of the melanoma monolayer. LuIII, however, effectively killed the entire melanoma culture at an input of 200 vge/cell, an input that initially leads to infection of about 5% of susceptible patient-derived melanoma cells, as discussed below. This demonstrates the ability of LuIII not just to infect melanoma, but also to replicate and spread through the culture, and identifies this virus as the optimal candidate for melanoma oncolysis in these two model systems.

Primary human melanomas vary in their responses to parvovirus infection

We next screened a subset of five of these viruses, MVMp, H1, LuIII, H3, and TVX, using this killing assay, across a panel of 13 patient-derived, very low-passage melanoma samples. Fig. 2A–C, shows representative assays from this screen, chosen to illustrate the three types of outcome observed, as discussed below. As observed with the stepwise-transformed cells, MVMp and H3 demonstrated no killing ability in any of the patient-derived cell lines. We concluded from this screen that LuIII, and less potently H1, are the most efficient at infecting freshly isolated human melanoma cells, as predicted by the two melanoma models; however, the individual outcomes observed across the entire panel of patient-derived cultures were more varied. The results of the screen divided the cell lines into three distinct groups. Three cell lines: YUSIT1, YURIF, and WW165 appeared to be completely resistant to all five serotypes of parvovirus, growing to confluent monolayers even after exposure to the highest MOI. Eight cell lines, YUSAC-2, YUMAC, YUDOSO, YUKSI, YUKIM, YUROL, YUPLA, and YUHEF, showed evidence of infection and killing by both H1 and LuIII at only the highest virus input, with a spotty, incomplete recovery of the monolayer after 6 days of infection. Finally, two cell lines, 501-Mel and MNT1, mirrored the stepwise models in their sensitivity to both H1 and LuIII viruses. H1 showed complete killing of the culture down to a starting input of 200 vge/cell, and evidence of killing at an input as low as 8 vge/cell. LuIII demonstrated complete killing starting from only 40 vge/cell, and disruption of the resulting monolayer at both 8 and 1.6 input genomes per cell. These data demonstrated that

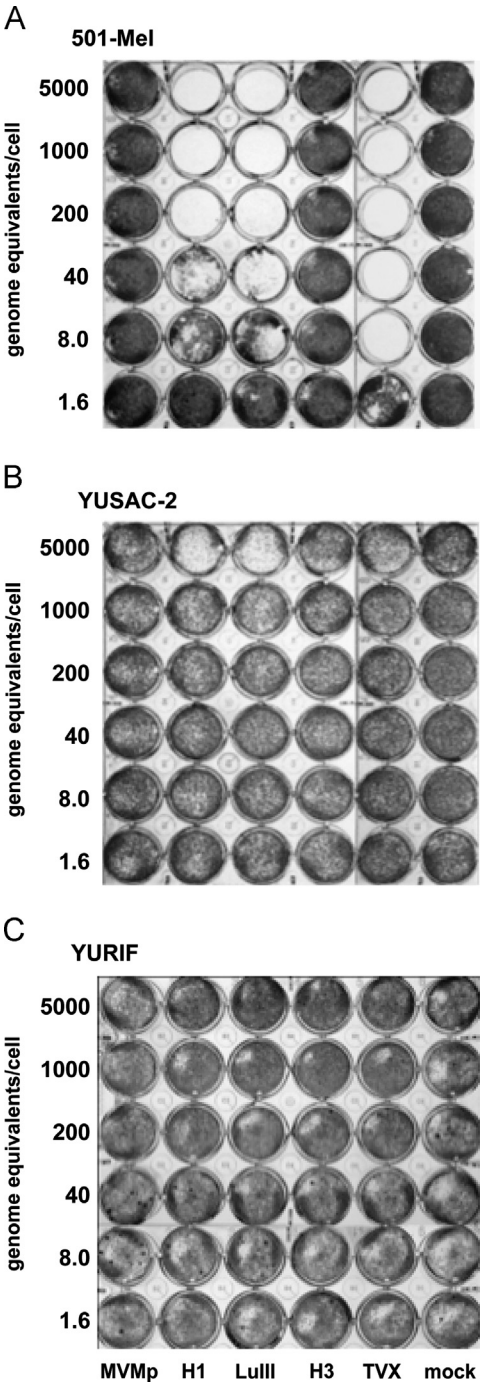

Fig. 2. Patient-derived melanoma cell lines respond to infection with three distinct outcomes. One representative is shown from each category of killing assay outcome —panel A, sensitive ($n=2$); panel B, intermediate ($n=8$); and panel C, resistant ($n=3$); the 13 patient-derived melanoma lines screened for parvovirus killing. Sub-confluent cells were infected with 5-fold serial dilutions of each virus and stained 6 days post-infection, as described in the Methods section.

the basic pattern of H1 and LuIII infectability seen in the stepwise melanoma models was reproduced in patient-derived cultures, with variability in the potency of the viruses in different cell lines, and confirmed that LuIII represents the best candidate, among the viruses tested, for parvoviral oncolysis of melanoma. Interestingly, one additional parvovirus serotype, TVX, a previously uncharacterized virus, demonstrated potency in the two most infectable cell lines, 501-Mel and MNT1, beyond that of either H1 or LuIII. However, TVX did not demonstrate any killing ability in either of the stepwise-transformed melanoma model (Fig. 1B and C), or in the other 11 clinical samples.

Given the three general outcomes observed in response to infection of the patient-derived cell lines, we wished to further explore differences in the LuIII lifecycle in these three groups. This approach was constrained by the fact that the majority of tools we have developed identify components of the prototype strain MVMp, a serotype unable to infect human melanoma cells. However, previous studies from our laboratory, of MVMp-resistant transformed human fibroblasts, showed that the LuIII VP2 capsid gene was sufficient to confer efficient infectivity on MVMp for this cell type (Paglino and Tattersall, 2011). We therefore compared the chimeric virus LuCap, in which the MVMp VP2 capsid gene has been replaced with that of LuIII (Fig. 3A), with both of its parents, using the 6-day killing assay in a representative clinical melanoma cell line from each sensitivity group. Fig. 3B shows that this virus does indeed demonstrate tropism for human melanoma cells, and kills these cells with nearly the same efficiency as the parent LuIII virus, allowing the study of parvovirus infection and killing of melanoma in the context of the prototype MVMp backbone. The further experimental analyses reported here were performed exclusively with LuCap.

The majority of melanoma lines support initiation of infection

Having identified LuCap as an optimal candidate for melanoma oncolysis, we focused on infection of the panel of patient-derived lines with this chimeric virus. First, the ability of LuCap to establish infection in 24 h was examined by measuring the expression of the early non-structural protein NS1 using flow cytometry. Analysis of the 13 cell lines revealed that a majority support initiation of infection by LuCap, as shown, in Fig. 4A, by a dose-responsive increase in NS1-positive cells with increasing input MOIs. For 10 of the cell lines between 12% and 70% of the cells became positive for NS1 when infected with 5000 vge/cell. The three cell lines, YUSIT1, YURIF, and WW165, that were found to be resistant to all the parvoviruses used in the initial screen also displayed essentially

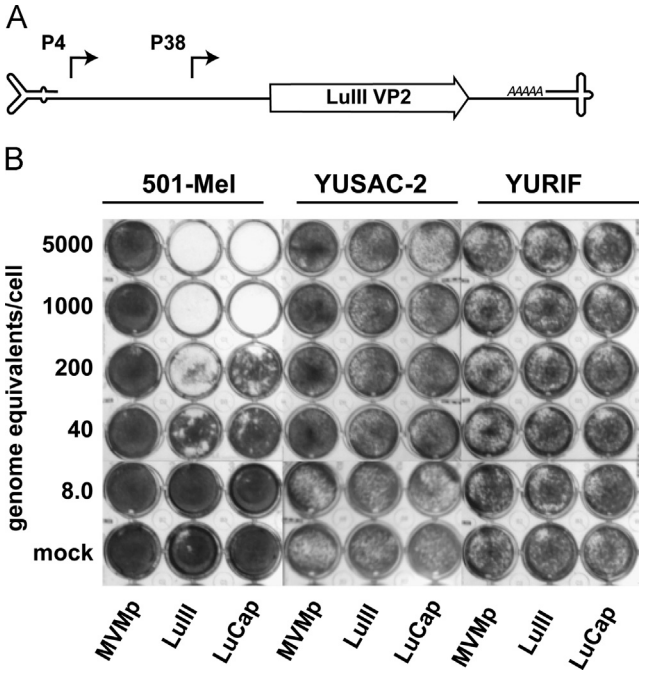

Fig. 3. The LuIII capsid gene confers melanoma tropism to MVMp. Panel A diagrams the chimeric virus LuCap, showing its MVMp genome backbone and the dispositions of both viral promoters, and the LuIII VP2 capsid gene replacing that of MVM. Panel B shows killing assays of representative patient-derived melanoma cell lines with the parent viruses MVMp and LuIII, and the LuCap chimera. Sub-confluent cells were infected and stained as described in the Methods section.

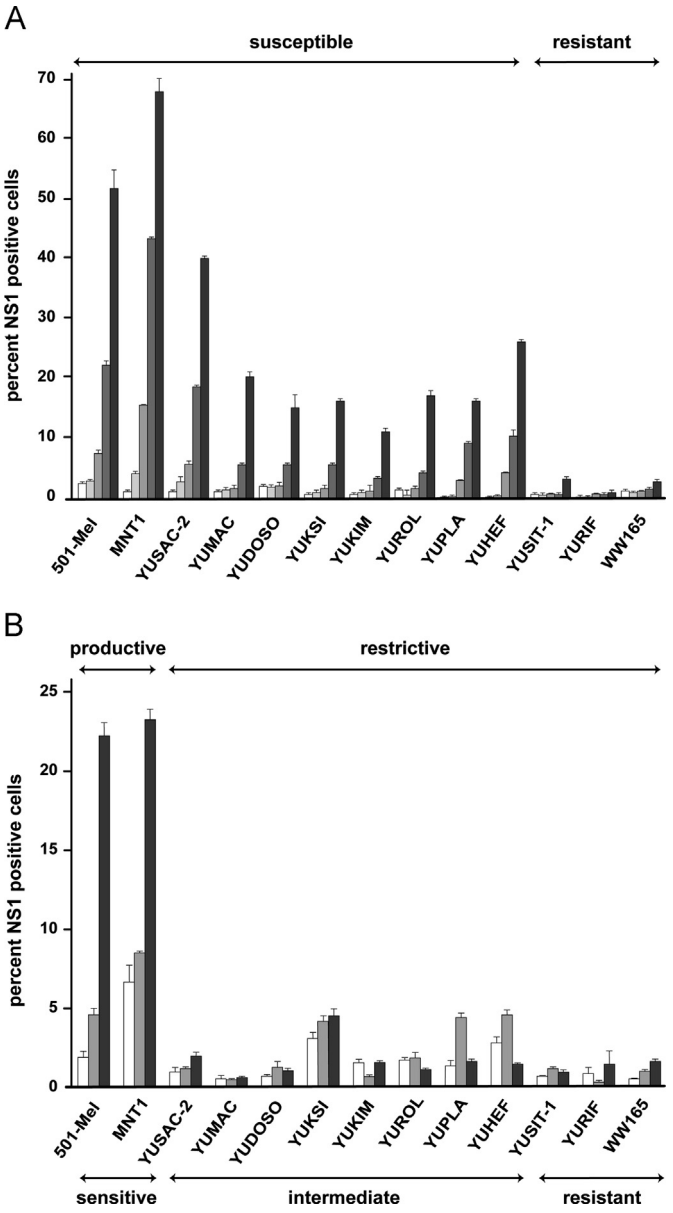

Fig. 4. Infection initiation and expansion of LuCap infection in patient-derived melanoma cell lines. Panel A shows a histogram representing the percent of cells expressing NS1 at 24 hpi, as measured by flow cytometry. The 13 cells lines, indicated at the bottom, were infected with LuCap virus at increasing MOIs, in 5-fold steps from 8 to 5000 vge/cell, as indicated by the shading intensity of the bars. Panel B shows a graphical representation of the percent of cells expressing NS1 as a function of time after infection, for cell lines initially infected at a single MOI of 100 vge/cell, collected at 24 h (white bars), 48 h (gray bars), and 72 h (black bars), and analyzed by flow cytometry.

complete resistance to the induction of NS1 expression by LuCap, even at the highest MOI used (Fig. 4A).

Next we measured the ability of LuCap to replicate productively and expand through dividing melanoma cultures over 72 h, following infection at an initially low MOI (100 vge/cell) (Fig. 4B). Again, the cell lines fell into two groups: those that support a productive, expanding infection, and those that do not. The 501-Mel and MNT1 support expansion, as the percentage of NS1-positive cells in these two lines increased from 2% and 6% at 24 h, to 22% and 24% at 72 h, respectively. This indicates that infected cells produce progeny virions that spread to infect additional cells in the culture, at a rate faster than the remaining uninfected cells can repopulate the culture. The remaining 11 cell lines failed to support a productive infection, showing no

significant increase in the percentage of infected cells by 72 h post-infection (hpi).

By superimposing the results for infection initiation and expansion in these cell lines, we clearly identify three overall infection outcomes, partitioning the cell lines into three subgroups: resistant (YUSIT1, YURIF, WW165), intermediate (YUSAC-2, YUMAC, YUDOSO, YUKSI, YUKIM, YUROL, YUPLA, YUHEF,) and sensitive (501-Mel, MNT1) (Fig. 4). The three cell lines in the resistant subgroup are not permissive to infection, or even the establishment of NS1 protein expression, in the initial infection. Members of the intermediate subgroup are permissive to infection, supporting at least the early stages of the viral lifecycle, including early gene expression; however, the lack of expansion suggests a late block in the lifecycle. Finally, the two cell lines in the sensitive subgroup are efficiently infected in the first round, and support a productive infection with expansion through the culture, as illustrated by the increase in the NS1-positive cells over time, and complete the destruction of the monolayer even at low input MOIs.

Human melanoma cell lines bind and internalize LuCap virions regardless of their infectability

Two representative cell lines were selected from each of these three subgroups for further analysis: sensitive 501-Mel and MNT1, intermediate YUSAC-2 and YUMAC, and resistant YURIF and WW165. To determine the step in the viral lifecycle at which infection is blocked in resistant cell lines, we first examined their ability to bind and internalize virus particles. Although the receptor(s) for MVM and LuIII remain uncharacterized, they contain an essential terminal sialic acid residue, as judged by the ability of neuraminidase treatment to reverse cell surface binding of either virus, and this property can be used to measure the kinetics and extent of virion binding and entry. Cells were infected for 4 h with LuCap virus, and then incubated for an additional 2 h either with neuraminidase, in order to measure virus particles that had been internalized, or without neuraminidase to assess total cell-associated virus. As a control, one sample from each cell line was treated with neuraminidase prior to infection, to confirm that the virus requires surface sialic acid moieties for entry into each of the cell lines. Following infection, parvoviral genomes in the cell lysates were measured by qPCR. In all cases, neuraminidase pre-treatment effectively blocked virus binding and uptake (Fig. 5). Each of the six cell lines showed an increase in qPCR signal following infection, indicating that all cell lines are capable of binding the virus. Notably, all cell lines, including the two resistant cell types retained most of this signal following neuraminidase cleavage of bound virus, demonstrating their ability to also internalize virus. Although the cell lines differed somewhat in the measured amount of internalized virus, there was no correlation between the infectability of subgroups and the amount of virus they internalized. Indeed, LuCap virions were able to bind to, and successfully enter, the resistant cells YURIF and WW165 to levels equivalent to, or even exceeding, those seen for permissive cells, indicating that the infection of these resistant cells is blocked at a post-uptake step.

Resistant cell lines are blocked for infection prior to viral gene transcription

Following internalization, trafficking of virus into the nucleus, and entry of the host cell into S-phase, the single-stranded viral genome is uncoated and converted to duplex DNA by host DNA polymerase, creating a transcription template, initially for mRNAs driven by the P4 promoter. We next looked for evidence of transcription of the earliest expressed genes, NS1 and NS2, in resistant cells infected with LuCap, since the failure to detect NS1 protein expression in resistant cells in the initiation assay does not rule out a post-transcriptional block to gene expression. To measure the amount of viral gene

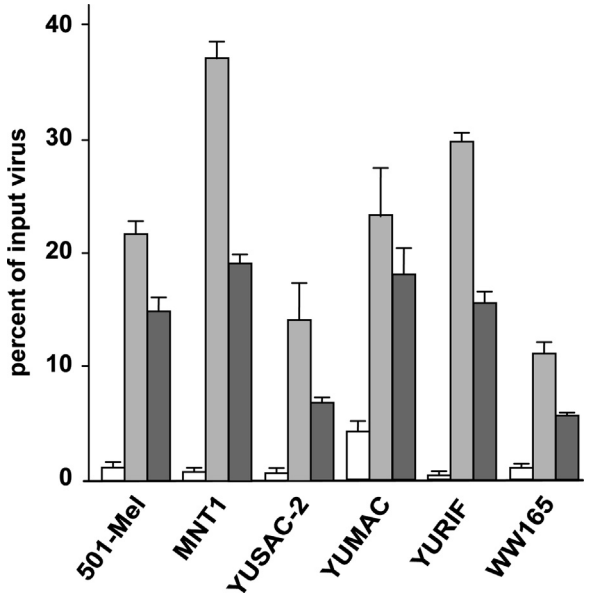

Fig. 5. Virion binding to, and occlusion by, patient-derived melanoma cells. Cells were infected for 4 h with LuCap virions, and incubated for a further 2 h to allow for recycling of virus from the cell. For the pre-cleaved samples (white bars), cells were incubated prior to infection with neuraminidase to prevent virus binding. For the occluded samples (light gray bars), cells were incubated for the final 2 h in neuraminidase-supplemented medium to cleave surface-bound virions, while for the "bound and occluded" samples (dark gray bars), neuraminidase was omitted in order to measure the total cell-associated virus. Cells were lysed at 6 hpi, and lysates were analyzed for virus genomes by qPCR. The percent uptake is calculated versus qPCR of the total input virus added to an uninfected lysate.

transcription from the P4 promoter, we measured the levels of R1 and R2 transcripts at 24 h after infection, using RT qPCR and a primer strategy indicated in Fig. 6A. As shown in Fig. 6B, each of the sensitive and intermediate cell lines transcribe both NS1 and NS2 genes, but the resistant cells did not support detectable transcription of either NS1 or NS2 genes, indicating that the competent P4 transcription complexes fail to form in these cells.

Since the intermediate cell lines expressed P4 transcripts abundantly, the next step in identifying the block to infection in these cells was to analyze the translation of viral transcripts, particularly those of the capsid genes VP1 and VP2, whose expression is dependent upon NS1 transactivation of the P38 promoter. For this, we infected all six representative cell types at a high MOI, and analyzed viral protein expression at 24 hpi by western blot. Sensitive and intermediate cells all expressed significant levels of NS1, and the capsid gene products VP1 and VP2 (Fig. 7). The ancillary protein NS2, which, as discussed above, has been found to be non-essential for the infection of several transformed human cells, was expressed at lower, more variable levels, reflecting the lower levels of the R2 transcript class that encodes them observed in Fig. 6B. Importantly, LuCap infection of intermediate cell lines led to significant accumulation of the viral capsid gene products, indicating that the block causing their failure to support a second round of infection operates after capsid gene expression.

Intermediate cell lines support viral DNA replication

In order for progeny viral particles to be generated, the viral genome must first be amplified as duplex DNA by rolling hairpin replication, nicked by NS1, and 5 kb single-stranded viral genomes displaced from these duplexes for packaging (Cotmore and Tattersall, 2005b). To measure DNA synthesis, the cells were infected under single-round conditions, intracellular DNA isolated at 6, 24 and 48 h, and analyzed by a qPCR assay that detects a viral DNA sequence within the NS1 gene (Fig. 8A). These results indicate that both sensitive and

intermediate cell lines support viral DNA replication. In 501-Mel cells, LuCap begins DNA replication rapidly, within 24 h, while MNT1 and YUSAC-2 lag behind, continuing to increase the rate of replication between 24 and 48 h. The intermediate cell line YUMAC also

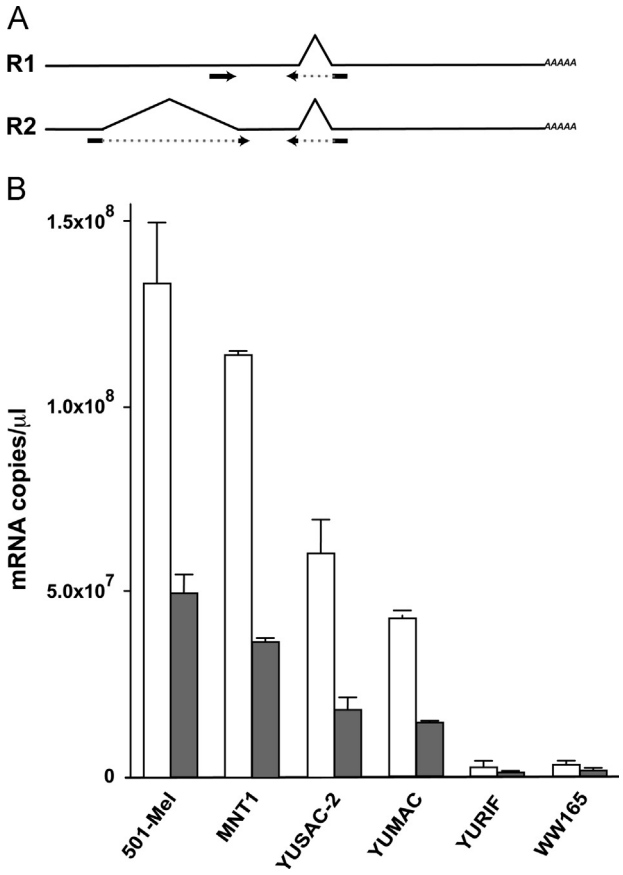

Fig. 6. Measurement of P4 promoter activity in representative melanoma cells. Panel A depicts the arrangement of the spliced transcripts and the primers used to detect them. For panel B, two representative cell lines from the three infectability subgroups were infected at high multiplicity and collected at 24 h for RNA isolation and cDNA synthesis. Viral R1 (NS1-encoding—white bars) and R2 (NS2-encoding—gray bars) transcripts were measured by SYBR Green qPCR, as described in the Methods section. Copy number was calculated by comparison to standard curves of NS1 and NS2 cDNA sequences.

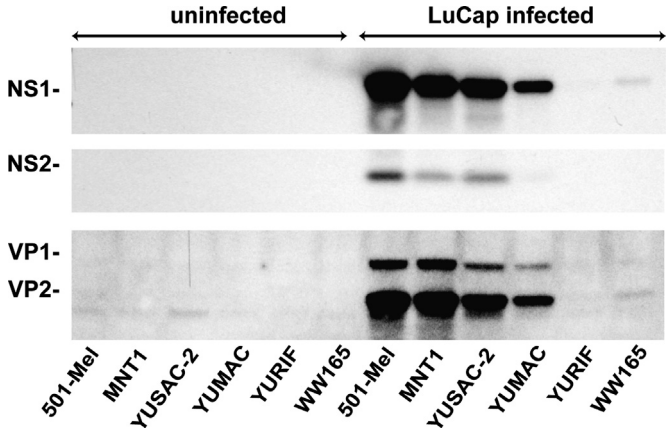

Fig. 7. Analysis of viral gene expression in representative melanoma cell infections. Six cell lines representing the three infectability subgroups were analyzed by western blotting following 24 h of infection at high multiplicity. Blots were probed for the products of the non-structural genes NS1 and NS2, and the capsid genes VP1 and VP2, using specific antibodies, as described in the Methods section.

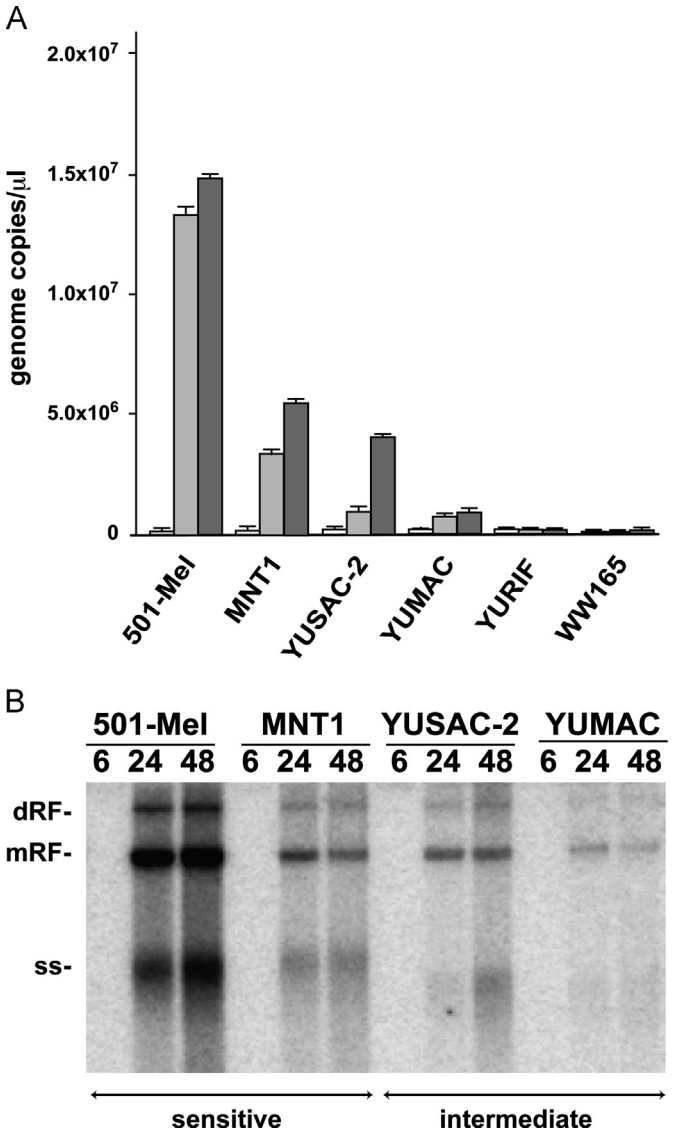

Fig. 8. Viral DNA replication in representative melanoma cell infections. Cells were infected at high multiplicity under single-cycle conditions. Intracellular DNA was isolated from cells at 6, 24 and 48 hpi. For panel A, viral DNA was measured by qPCR for all six cell lines, with copies quantified by comparison to a standard curve of LuCap plasmid DNA. For panel B, 10 kb dimer (dRF) and 5 kb monomer (mRF) replicative forms of viral DNA, and single-stranded progeny viral genomes (ss), isolated from infected sensitive and intermediate cells, were separated by size in a neutral gel and analyzed by Southern blot, as described in the Methods section.

demonstrates replication, though at a slower rate than the others. Finally, the two resistant cell lines failed to replicate viral DNA, as was expected in the absence of NS1 expression, the viral protein critical for genome replication. These cell lines were not, therefore, included in subsequent analyses of the viral replication cycle. The qPCR approach to measuring genome amplification, however, does not elucidate the state of the replicating DNA, since 5- and 10-kb duplex replicative forms, single-stranded, packaging-competent genomes, and hybrid replicative intermediates are all detected as a single signal. To detect these different replicative forms and to determine whether single-stranded genomes were being released, we separated the DNA by size on a neutral gel, and detected viral DNA by Southern blot (Fig. 8B). These data demonstrate that both intermediate cell lines successfully replicate viral DNA, and accumulate intracellular single-stranded 5 kb genomes, though at a significantly lower rate than the sensitive 501-Mel cell line. Interestingly, the sensitive cell line MNT1, which supports both initiation and expansion of LuCap at slightly higher levels than

seen in 501-Mel (Fig. 4), replicates viral DNA significantly less effectively than 501-Mel, in fact demonstrating the same level of replication as the intermediate cell line YUSAC-2, a cell line which fails to support viral expansion. Therefore, the decreased rate of DNA replication demonstrated by the intermediate cell lines does not alone account for the late block to infection, since the decreased rate of replication in MNT1 does not hinder rapid expansion of LuCap infection in cultures of this cell line.

Intermediate cell lines assemble viral capsids correctly

Capsid protein analysis by western blot does not give information about the ability of cells to assemble the capsid protein monomers into three-dimensional capsids. In order to assess capsid assembly, we infected cells for 48 h at a high MOI, and separated cell lysates by density on iodixanol gradients, and analyzed fractions from this gradient for the presence of capsid proteins by western blot, as shown in Fig. 9A. In the fractionation of sensitive cell extracts, the bulk of viral capsid protein forms a peak centered on fraction 7, in the position of assembled, but empty, particles. Full particles, containing the viral genome, would be expected to band between fractions 3 and 4, but have not accumulated levels detectable by western blot by this point in infection, at least as intracellular particles. The intermediate cell lines YUSAC-2 and YUMAC appear to assemble capsids nearly as efficiently as the sensitive lines 501-Mel and MNT1, showing a similar pattern, with capsid proteins banding in the empty particle region of the gradient. For both sensitive and intermediate cell infections, the capsid distribution in these gradients coincides with the peak of hemagglutination activity, which is a property of assembled capsids. Thus, the failure of the intermediate cells to support multiple rounds of infection does not result from a failure to assemble capsids correctly, and must instead be based on deficient packaging or release of progeny virus from infected cells.

Intermediate cell lines fail to export progeny rapidly

Since intermediate cell lines generate single-stranded genomes during viral DNA replication and assemble VP1 and VP2 proteins into capsids, the next step was to determine whether these genomes were being packaged into the assembled capsids. To this end, we analyzed the fractions in the region of the iodixanol gradients where packaged virions band for viral DNA. To definitively determine whether the viral DNA was packaged into capsids, any uncoated DNA was digested with micrococcal nuclease. Additionally, to measure the amount of progeny virions released into the medium over the 48 h infection, we digested any unencapsidated DNA in the medium with micrococcal nuclease, and concentrated the sample prior to alkaline gel electrophoresis and Southern blot analysis (Fig. 10A). Intracellular encapsidated viral DNA was present in all four cell lines, and peaked at fraction 3, indicating the ability of both intermediate cell lines to package progeny virions. Surprisingly, the amount of full particles in the sensitive cell line MNT1 was far lower than that of the sensitive line 501-Mel, and further was significantly below the amount of packaged intracellular progeny found in the intermediate cell line YUSAC-2. However, the analysis of extracellular virus demonstrates that both sensitive cell lines effectively export packaged progeny virions out into the medium, as that is where the vast majority of signal is found. This explains both the low levels of intracellular single-stranded progeny DNA seen in Fig. 8B, and the absence of capsid proteins or hemagglutinin detectable at the position where full virions would band in the gradients shown in Fig. 9. The medium from both intermediate cell lines also contained progeny virions, but in much lower abundance compared to either sensitive cell line. Comparison of the quantified bands

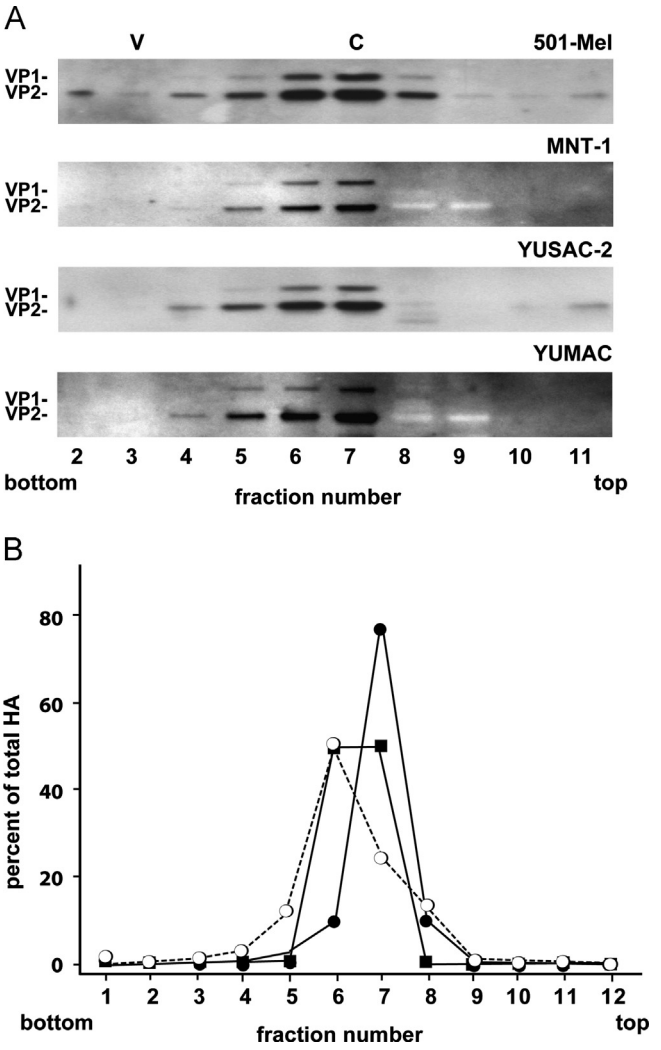

Fig. 9. Capsid assembly in representative melanoma cell lines. Sensitive and intermediate cell line representatives were infected at high multiplicity under single-cycle conditions. Cell lysates were prepared at 48 h and centrifuged through an iodixanol step gradient to separate viral particles by density, as described in the Methods section. Fractions are numbered from the bottom of the gradient, and the banding positions of full virions (V) and empty capsids (C) are indicated. In panel A, each fraction was analyzed by western blot for capsid genes VP1 and VP2, and in panel B, hemagglutination (HA) assays were performed on each fraction for the two intermediate cell lines, YUSAC-2 (●) and YUMAC (■), and compared to those for the sensitive cell line 501-Mel (◯). Titers are expressed as a percent of the total HA recovered from each gradient.

revealed that sensitive cell lines export 25–30 times more progeny virions into the medium than they contain intracellularly, whereas, for the intermediate cell lines, this ratio is only 6–7 (Fig. 10B). Thus, the early progeny release from the sensitive cell lines likely represents the key factor allowing for rapid expansion through the culture, at a rate sufficient to overwhelm even a rapidly growing cell population.

Permissive cell lines die as a consequence of infection

While it is clear that a majority of the melanoma lines are infectable with the LuCap virus, it was important to determine the outcome of infection, particularly for the intermediate cell lines that are permissive to LuCap virus, but fail to amplify the infection. To study this, cells infected under single-round conditions were harvested at 24, 48, and 72 h and stained for dead or dying cells, as described in the Methods section. For this, infected monolayers were stained with a cell-impermeant dye which, while fluorescently staining surface

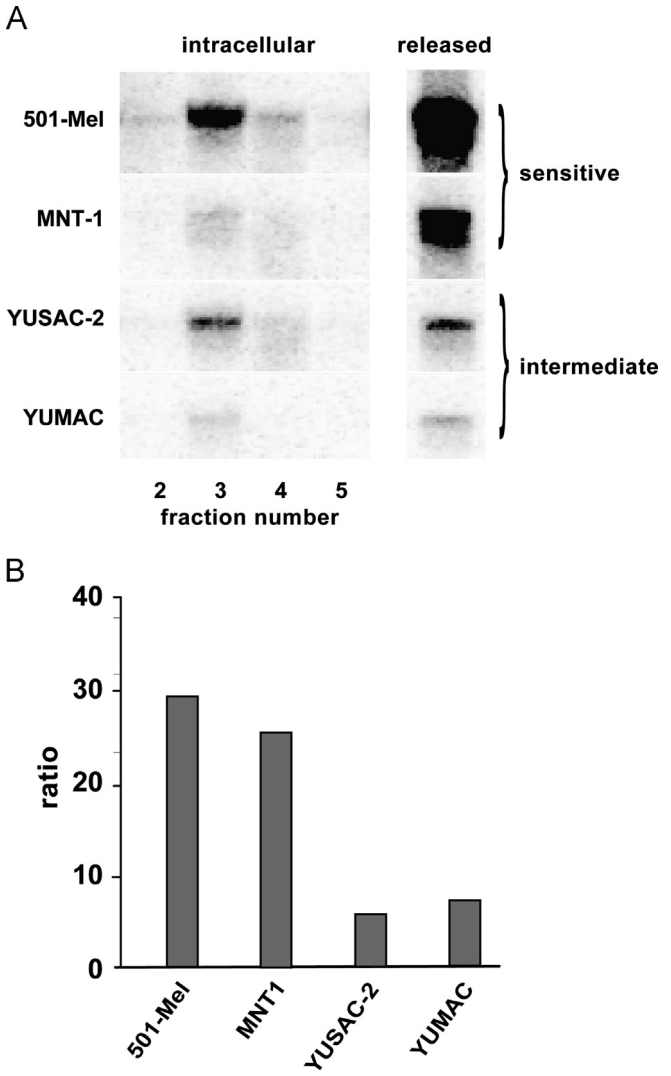

Fig. 10. Progeny genome packaging in representative melanoma cell infections. Panel A: lysates of cells infected for 48 h were fractionated by density as described in Fig. 9. Samples from indicated fractions were treated with micrococcal nuclease to cleave un-encapsidated DNA. Protected, packaged 5 kb DNA was then electrophoresed on an alkaline gel, and analyzed by Southern blot. The intracellular fractions represent 60% of the total volume of each fraction, whereas released samples represent micrococcal nuclease-protected virus genomes in concentrated extracellular medium, representing 10% of the total medium volume. Panel B: quantified bands were corrected for their representative volumes, and resulting ratios represent the amount of packaged DNA in the medium compared to the amount of packaged DNA in fraction 3, for each cell line.

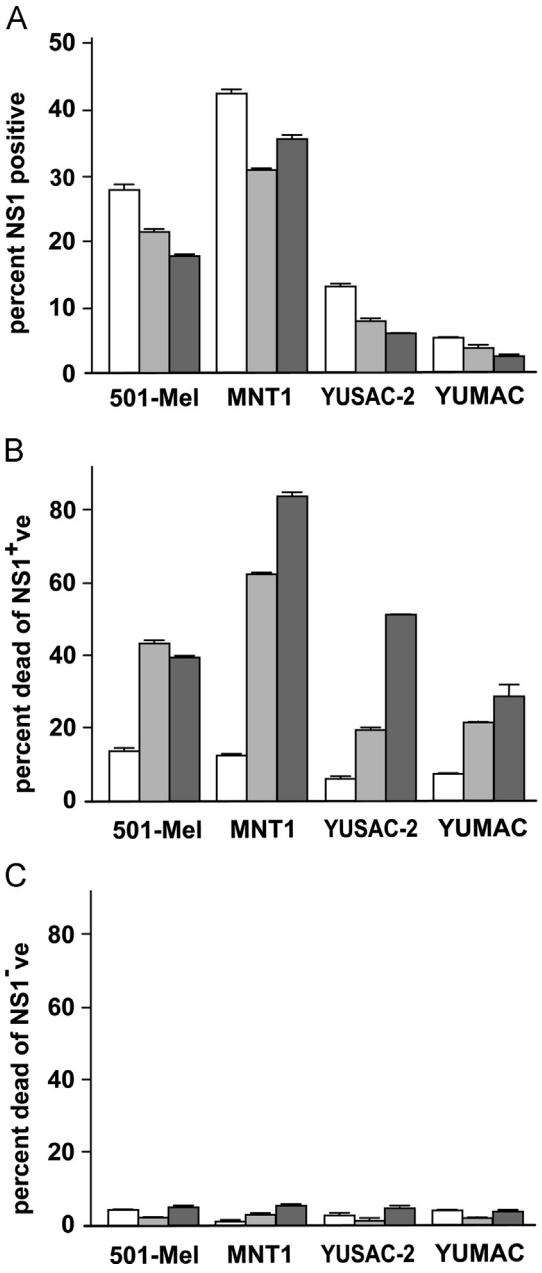

Fig. 11. Analysis of the fate of representative melanoma cells following infection. Sensitive and intermediate representative cell lines were infected with 1000 vge/cell, under single-cycle conditions. Cells were collected at 24 hpi (white bars), 48 hpi (light gray bars) and 72 hpi (dark gray bars), and stained for plasma membrane integrity and NS1 expression, as described in the Methods section. Panel A shows the percent of cells infected (NS1-positive) at each time point. Panels B and C show the percent of NS1-positive and NS1-negative cells, respectively, that are also positive for the high intensity staining that indicates loss of plasma membrane integrity.

moieties on intact cells, stains those that have lost plasma membrane integrity with one to two orders of magnitude greater intensity. After removal of the dye and washing, the cells were fixed, permeabilized and co-stained with antibody to viral NS1 to identify infected cells, then analyzed by flow cytometry. Fig. 11A shows the percent of cells positive for NS1 at the three time points. In each case, the percent infected decreased over time, presumably due to neuraminidase-mediated inhibition of second round infection and the continued division of uninfected cells. To determine the fates specifically of infected cells, we gated on NS1-positive cells and analyzed the percent positive for the intense fluorescence marker of cell death. As shown in Fig. 11B, for both sensitive and intermediate cell lines the percent of dead and dying infected cells increased over the course of the experiment, indicating that the infection was inducing cell death irrespective of whether the infection was productive or restrictive. To control for the normal occurrence of cell death in culture, we also measured the percent of dead cells after gating on the uninfected population. Fig. 11C shows that this percentage did not increase over time, confirming that the dying and dead cells in each of the cultures were losing their plasma membrane integrity as a direct result of virus infection, independent of their ability to sustain an expanding infection.

Discussion

In this study, we identified LuIII as the parvovirus with the greatest potential for infecting and killing the majority of primary human melanomas tested, with the LuIII VP2 capsid gene being

sufficient to confer melanoma tropism to the otherwise ineffective virus MVMp. LuCap was able to initiate infection, demonstrated by the expression of NS1, in 10 of 13 very low-passage, patient-derived melanoma cell lines.

A minority of human melanomas are resistant to rodent parvovirus infection

Three of the tested melanoma lines failed to support initiation of infection, blocking the virus at an early step, prior to gene expression, but after uptake into the host cell. Between these two stages, the virus must escape the endosome, traffic to and enter the nucleus, and release its single-stranded genome, which must be converted to a double-stranded form, by host DNA polymerase, and establish itself as a competent transcription template. Infection may be blocked at any one of these steps in resistant cells; however, the successful trafficking of a virus to the nucleus appears to be a rare event even in permissive cells, demonstrated by high particle-to-infectivity ratios, variously estimated at 300:1 for MVMp, 1000:1 for CPV, and 500–1000:1 for H1 (Cotmore and Tattersall, 2007; Paradiso, 1981), a fact that greatly complicates effective analysis of these early steps of the virus lifecycle. Thus, at this time, the block to infection in resistant cell lines can only be identified as occurring at a post-uptake, pre-transcriptional step. Similar early, post-entry blocks have been reported frequently for parvovirus infections, and, in some cases, have been found to map to the capsid gene (Bergeron et al., 1996; Bloom et al., 1993; Paglino and Burnett, 2007; Paglino and Tattersall, 2011; Parrish and Carmichael, 1986). Capsid-mediated blocks can often be overcome by transfection of the infectious clone, resulting in the progression of the virus lifecycle (Gardiner and Tattersall, 1988; Previsani et al., 1997). However, the resistant melanoma cell lines described in the current study proved exceedingly difficult to transfect, failing to express a control gene under a variety of transfection conditions, so we cannot yet determine whether bypassing the early, post-uptake role of the virus capsid would result in gene expression and DNA replication in these cell lines. If this were found to be the case for these resistant melanomas, it would indicate that an alternative capsid might be employed to confer viral infectivity against the resistant cells.

Most human melanomas are killed by rodent parvovirus infection

Of the 10 cell lines that supported infection, only two efficiently supported multiple cycles, allowing the infection to spread over time. The remaining eight intermediate cell lines failed to generate and export sufficient progeny to sustain the infection, but nevertheless died as a result of the initial infectious event. Investigation of similar blocks to parvovirus infection in other systems points to a role for the non-structural genes in determining successful oncotropism at this later stage of infection (Choi et al., 2005; Eichwald et al., 2002; Rubio et al., 2001). For instance, MVMi infection of human astrocytic tumors uncovered two types of late blocks. Infection of U87 cells failed to proceed to viral DNA replication, despite conversion of the genome to a double-stranded form, and robust viral protein expression. On the other hand, infection of U373 cells was restricted by weak production and release of infectious progeny, despite efficient protein expression and DNA replication. The latter block was overcome by exchanging a portion of the MVMi non-structural gene sequence with that from MVMp, which is not restricted for growth in these cells (Rubio et al., 2001). Additionally, when MVMi DNA was transfected into murine fibroblasts, in order to bypass its capsid-mediated restriction in this cell type, the virus failed to produce progeny genomes efficiently. However, changing a single, non-coding nucleotide within the major intron splice acceptor site to that present in MVMp results in an increase in the relative levels of R2 transcripts, which encode NS2, and leads to robust progeny genome production and packaging (Choi et al., 2005). Thus the requirements for relative amounts of the NS splice variants can play a major role in late stages of the virus lifecycle, can vary from cell to cell, and between host species. While the requirement for NS2 in murine cells appears to be absolute, expression of this ancillary protein appears to be dispensable for efficient infection of many transformed human cells (Cotmore et al., 1997; Naeger et al., 1993, 1990), suggesting that a dysfunction of NS1, rather than NS2, may be involved in the late block in the human melanoma cells studied here. If NS1 is indeed involved in the late block, it stands to reason that an appropriate chimeric virus, encoding both melanoma tropic capsid and NS genes, could confer the ability to efficiently export packaged progeny from infected cells, to aid in rapid expansion through the culture, although recent studies suggest that this may not be an important factor in cancer virotherapy.

Parvoviral oncolysis might require cell killing, rather than expansion of infection

While an expanding infection would be optimal for infecting the bulk of cells in a tumor, in practice it may not be necessary for therapeutic efficacy in vivo. The majority of melanoma lines supported at least initiation of infection, and regardless of the ability to produce progeny for additional rounds, infection invariably ended in the death of the infected cell. This finding is critical in that it indicates that even cancers that support only a single round of virus-induced cell death might still be susceptible to the immunological sequelae of parvovirus infection. Some chemotherapeutic agents (e.g. anthracyclines, oxiplatin, and oxidizing radiation) owe a significant portion of their outstanding efficacy to the fact that cancer cells treated with them die by a process described as immunogenic cell death, priming the adaptive immune system for cytotoxic T cell-mediated destruction of residual chemotherapy-resistant cells (Zitvogel et al., 2008). Parvovirus infection of tumor cells has also demonstrated the activation of an anti-tumor immune response in both human tumor lines in vitro and mouse models in vivo (Bhat et al., 2011; Grekova et al., 2012, 2011; Raykov et al., 2007). In one of these studies, immunocompetent mice challenged with MVM-infected glioma were fully protected from tumor growth, while only 20% of immunodeficient mice demonstrated protection (Grekova et al., 2012). Therefore, while an expanding infection may increase the number of tumor cells infected, immunogenic death of cells that can only sustain a single round of infection might still promote the activation of an anti-tumor immune response, leading to the targeted immune destruction of cells far beyond the scope of those initially infected.

Parvoviruses could also be used as adjuvants to more conventional therapy, and have demonstrated the potential to target cancer cells with acquired resistance to chemotherapy. Malignant cells often up-regulate survival signals that render them unresponsive to the activation of death pathways triggered by chemotherapy. However, parvovirus-mediated death can occur via a range of pathways depending on the virus serotype and host, with caspase-dependent apoptosis, p53-independent apoptosis, and necrosis all having been described (Mincberg et al., 2011; Moehler et al., 2001; Ran et al., 1999; Rayet et al., 1998). For instance, glioma cells resistant to both TRAIL- and cisplatin-mediated death due to an over-expression of Bcl-2 family survival signals were successfully killed by H1-mediated activation of an alternative, cathepsin-mediated death pathway (Di Piazza et al., 2007).

In conclusion, we found that a chimeric parvovirus, LuCap, can infect a majority of freshly isolated, patient-derived malignant melanoma cell lines, resulting in their death. Current understanding of the therapeutic importance of the activation of an anti-tumor immune

response, and the ability of parvovirus-induced cell death to stimulate such a response, strongly indicates that parvoviral therapy of malignant melanoma merits further study. We suggest that a single round of infection with ensuing cell death might be sufficient for a therapeutic response in vivo, particularly if combined with the delivery of immunomodulatory gene products, or with antibody-mediated immunotherapy. Further study of the blocks to infection in both resistant and intermediate cell lines may elucidate strategies for circumventing them, thus further optimizing infection and therapeutic efficacy.

Materials and methods

Cells

Low-passage, patient-derived melanoma cell lines were provided by Antonella Bacchiocchi in the Specimen Research Core of the Yale Specialized Program of Research Excellence (SPORE) in Skin Cancer, and cultured as described by Tworkoski et al. (2011), in Opti-MEM (Invitrogen, Grand Island, NY) containing 5% fetal bovine serum (FBS), and 1% glutamine, penicillin, and streptomycin. The stepwise-transformed melanoma models Mel-STR (Gupta et al., 2005) and pMel-TCP-BRAF (Garraway et al., 2005) were the kind gifts of Dr. Robert Weinberg (Whitehead Institute for Biomedical Research) and Dr. David Fisher (Harvard Medical School), respectively. Both cell lines were grown in DMEM containing 10% fetal bovine serum, and 1% glutamine, penicillin, and streptomycin.

Viruses

All virus stocks were grown in HeLa cells or in NB 324 K cells (simian virus 40-transformed human newborn kidney cells), and purified on step-gradients of iodixanol (Optiprep, Axis-Shield, Oslo, Norway) as previously described (Cotmore et al., 2010). Titers reflect encapsidated viral genomes, as quantitated by Southern blot following micrococcal nuclease digestion and alkaline gel electrophoresis. The probe used was the oligonucleotide 5′-AACTTTCCATTTAATGACTGTACCAACAA-3′, representing a DNA sequence in the helicase domain of NS1 that is conserved throughout the rodent parvoviruses, labeled at its 5′-end with ^{32}P-ATP using polynucleotide kinase, as described previously (Cotmore and Tattersall, 2005a).

Cell killing assay

Ten thousand cells were seeded overnight in a 1 ml volume per well in 24-well plates. Viruses were serially diluted 1:5 in growth medium beginning with a multiplicity of infection (MOI) of 5000 viral genome equivalents (vge) per cell, added as a 500 μl inoculum directly to the medium in each well. After 6 days of incubation at 37C, the medium was removed, and cells were fixed in Leishmann's stain.

Infection initiation assay

Two hundred thousand cells were seeded overnight in 2 ml of medium per well in a 6-well plate. Virus was diluted to the desired concentration in growth medium, added in a 500 μl volume directly to the medium in each well, and incubated at 37 °C. After 24 h of infection, medium was transferred to a collection tube, cells were harvested by trypsinization, and collected into the medium. Cells were then pelleted at 400 × g for 3 min (the same parameters were used for all subsequent spins), and fixed in 1% paraformaldehyde in FACS buffer (1% FBS in PBS) for 30 min at 4 °C, washed once with FACS buffer, and blocked for 30 min in FACS buffer containing 10% BSA. Cells were stained for NS1 with the mouse monoclonal antibody CE10B10 (Yeung et al., 1991) in iFACS buffer (1% FBS, 1% Saponin in PBS) for 1 h at 4 °C, washed twice with iFACS buffer, then stained for 1 h at 4 °C with Alexa-Fluor 488-conjugated goat anti-mouse IgG (Invitrogen) secondary antibody. Stained cells were analyzed on a FACSCalibur flow cytometer (Becton Dickinson, Franklin Lakes, NJ), using gating values established with infected cells, prepared as described above, but without incubation with the primary antibody. Results are expressed in histogram form with error bars that represent the standard deviation of the mean for duplicate infections.

Infection expansion assay

Two hundred thousand cells per well were seeded overnight in a 6-well plate. Cells were infected with 100 vge/cell as described in the initiation assay, and collected for staining at 24, 48, and 72 h. Following tryspinization and fixation, cells were washed twice with FACS buffer and stored in 200 μl FACS buffer at 4 °C until all samples were collected. Cells were stained for NS1 as described in the initiation assay.

Virus internalization assay

One hundred thousand cells per well were seeded overnight in a 24-well plate in 1 ml of medium. "Pre-cleaved" control cells were pre-incubated for 30 m with 200 μl neuraminidase-supplemented growth medium, then infected for 4 h with 10^8 total viral genomes in neuraminidase-supplemented medium, followed by a 2 h incubation in neuraminidase-supplemented growth medium. To measure binding and uptake, cells were infected with 10^8 total genomes for 4 h, followed by a 2-h incubation in growth medium. To measure virus occlusion, cells were infected with 10^8 total genomes for 4 h, followed by a 2-h incubation in neuraminidase-supplemented growth medium. All wells were washed twice with 1 ml PBS, and covered with 100 μl of DirectPCR lysis buffer (Viagen, Los Angeles, CA). Total input virus was measured by adding 10^8 total LuCap genomes to the lysis buffer in an uninfected well. The plate was incubated overnight at 45 °C, and then 85 °C for 45 min. Lysates were used at a 1:10 dilution in a quantitative TaqMan qPCR assay for viral genomes Paglino et al., (2007) with the outside primers OK reverse 5′-CCCATTCCATGTCCTCGC-3′ and OK forward 5′-GCAGGAG GACGAGCTGAAAT-3′ and the FAM-labeled probe 5′-FAM-TCCCAAG TAGTTTCCGCTCCTCGTTGTAAA-TAMRA-3′, and analyzed with a Realplex Mastercycler (Eppendorf, Hauppauge, NY).

Analysis of viral gene transcription

Two hundred thousand cells were seeded overnight in 2 ml of growth medium per well in a 6-well plate. Growth medium was replaced with 1 ml of infection medium containing 5000 vge/cell of LuCap virus for 4 h at 37 °C, and then replaced with 2 ml of neuraminidase-supplemented growth medium for an additional 20 h. RNA was harvested according to the RNeasy kit (Qiagen, Santa Clara, CA) with an on-column DNA digestion according to the RNase-Free DNase Set instructions (Qiagen), and cDNA was synthesized using a ProtoScript M-MuLV First Strand cDNA Synthesis Kit (New England BioLabs, Beverly, MA), from 1.0 μg of total RNA, to yield a final volume of 50 μl. cDNA was used at a 1:10 dilution in a SYBR Green qPCR assay (SABiosciences, Frederick, MD). Oligonucleotide primer pairs that bind exclusively to cDNAs from spliced R1 and R2 transcripts were as follows: R1 (NS1-encoding) transcripts were amplified with the forward primer R1-FOR 5′-CCAACTCCTATAAATTTACTAG-3′ and the reverse primer SPL-REV 5′-ACCAAGTGATTTCAGGCCTTAG-3′. R2 (NS2-encoding) transcripts were amplified with the forward primer R2-SPL-FOR 5′-GATGAAATGACCAAAAAGGTTC-3′ and the reverse primer SPL-REV.

Analysis of viral gene expression

Cells were seeded and infected as described for above transcription analysis. Cell were lysed and quantified with a Pierce BCA Protein Assay Kit (Thermo Scientific) as previously described (Ruiz et al., 2011). About 50 μg aliquots (with 100 mM DTT and loading dye) were loaded in a 4–20% Mini-Protean TGX Gel (Bio-Rad, Hercules, CA), and transferred to a Hybond ECL membrane (GE Healthcare). Membranes were blocked, incubated with a rabbit antibody directed against MVM NS1/2 N-terminal peptide (Cotmore and Tattersall, 1986) for the non-structural proteins, or the "LUCAPS" rabbit antibody directed against the capsid gene products VP1 and VP2 (Paglino and Tattersall, 2011), and developed using an ECL system according to the manufacturer's instructions (Amersham, Uppsala, Sweden).

Analysis of viral DNA replication

Cells were seeded and infected as described for capsid assembly. Cells were collected by trypsinization at 6, 24, and 48 h, and DNA was extracted from cell pellets as previously described (D'Abramo et al., 2005). DNA was first quantified by qPCR using a TaqMan assay as described for the internalization assay. To distinguish between replicative forms, and single-stranded forms of DNA in these samples, the DNA was separated by size in a 1.4% neutral agarose gel by electrophoresis, and detected by Southern blot analysis as before.

Capsid assembly and genome packaging

Five hundred thousand cells were seeded overnight in 5 ml growth medium in a 60 mm dish. Cells were infected with 1000 vge/cell in 1 ml of infection medium, and incubated at 37 °C for an additional 44 h in 5 ml of neuraminidase-supplemented growth medium. Cells were collected into the medium by scraping, pelleted at 2000 × g for 10 min, resuspended in 120 μl of 50 mM Tris–HCl, 0.5 mM EDTA, pH 8.7 (TE8.7), then frozen and thawed three times. Cell debris was pelleted at 2000 × g for 10 min, and 100 μl of cleared cell lysate was centrifuged through a small-scale (1 ml) iodixanol step gradient, as previously described (D'Abramo et al., 2005) modified to contain: 96 μl of 55%, 191 μl of 45 and 35%, and 96 μl of 15% iodixanol. Fractions were collected from the top of the tube in 50 μl aliquots, with the final aliquot being designated fraction #1. About 5 μl of each fraction was analyzed for capsid proteins by western blot as described above for the analysis of viral gene expression. Encapsidated DNA was detected by Southern blot following micrococcal nuclease digestion and alkaline gel electrophoresis as previously described (Farr and Tattersall, 2004). To measure the release of progeny virions, extracellular medium was treated with micrococcal nuclease digestion as previously described (Farr and Tattersall, 2004). Virions were concentrated from the medium by precipitating overnight at −20 °C in three volumes of 100% ethanol, pelleting at 14,000 rpm for 30 min, washing twice with 70% ethanol, and eluting with H_2O prior to running on an alkaline gel. Probed blots were analyzed on a Typhoon Trio variable-mode imager (GE Healthcare, Piscataway, NJ) using ImageQuant TL 7.0 image analysis software.

Measurement of virus-induced cell death

Two hundred thousand cells were seeded per well overnight in 2 ml of medium in a 6-well plate. Growth medium was replaced with 1 ml of infection medium (Opti-MEM supplemented with 1% FBS and 20 mM HEPES, pH 7.3) containing 1000 vge/cell of LuCap virus for 4 h at 37 °C. Inoculum was then removed and replaced with 2 ml of neuraminidase-supplemented (0.1 g/ml) growth medium for the remainder of the experiment to restrict the infection to a single round. Cells and medium were collected as described in the initiation assay, and washed once with 1 ml PBS. Cells were stained with the far red LIVE/DEAD Fixable Dead Cell Kit (Invitrogen) and fixed according to the manufacturer's instructions. Cells were resuspended in FACS buffer and stored at 4 °C until all time points had been collected (24, 48 and 72 h), then stained for NS1 as described in the initiation assay, and analyzed by flow cytometry.

Acknowledgments

Primary human melanoma cell lines were provided by the Specimen Core of the Yale SPORE in Skin Cancer, and we are grateful to Antonella Bacchiocchi and Ruth Halaban for advice on their culture. We thank Robert Weinberg and David Fisher for providing the Mel-STR and pMel-TCP-BRAF cell lines, respectively. We are indebted to Marcus Bosenberg and Susan Cotmore for critical advice, and the members of the laboratory for discussion and support. This work was supported, in part, by R01 CA029303 (P. Tattersall, PI) and by a DRP award from the Yale SPORE in Skin Cancer, P50 CA121974 (R. Halaban, PI), both funded by the National Cancer Institute. E.M.V. also received partial support from the Yale Medical Scientist Training Program, T32 GM007205 (J. Jamieson, PI).

References

Bergeron, J., Hébert, B., Tijssen, P., 1996. Genome organization of the Kresse strain of porcine parvovirus: identification of the allotropic determinant and comparison with those of NADL-2 and field isolates. J. Virol. *70*, 2508–2515.

Bhat, R., Dempe, S., Dinsart, C., Rommelaere, J., 2011. Enhancement of NK cell antitumor responses using an oncolytic parvovirus. Int. J. Cancer *128*, 908–919.

Bloom, M.E., Berry, B.D., Wei, W., Perryman, S., Wolfinbarger, J.B., 1993. Characterization of chimeric full-length molecular clones of Aleutian mink disease parvovirus (ADV): identification of a determinant governing replication of ADV in cell culture. J. Virol *67*, 5976–5988.

Chin, L., Watson, I.R., Kryukov, G.V., Arold, S.T., Imielinski, M., Theurillat, J.-P., Nickerson, E., Auclair, D., Li, L., Place, C., et al., 2012. A landscape of driver mutations in melanoma. Cell *150*, 251–263.

Chin, L., Garraway, L.A., Fisher, D.E., 2006. Malignant melanoma: genetics and therapeutics in the genomic era. Genes Dev. *20*, 2149–2182.

Choi, E.-Y., Newman, A.E., Burger, L., Pintel, D., 2005. Replication of minute virus of mice DNA is critically dependent on accumulated levels of NS2. J. Virol. *79*, 12375–12381.

Cornelis, J.J., Chen, Y.Q., Spruyt, N., Duponchel, N., Cotmore, S.F., Tattersall, P., Rommelaere, J., 1990. Susceptibility of human cells to killing by the parvoviruses H-1 and minute virus of mice correlates with viral transcription. J. Virol. *64*, 2537–2544.

Cotmore, S.F., Tattersall, P., 1986. Organization of nonstructural genes of the autonomous parvovirus minute virus of mice. J. Virol. *58*, 724–732.

Cotmore, S.F., Tattersall, P., 2005a. Encapsidation of minute virus of mice DNA: aspects of the translocation mechanism revealed by the structure of partially packaged genomes. Virology 336, 100–112.

Cotmore, S.F., Tattersall, P., 2005b. Genome packaging sense is controlled by the efficiency of the nick site in the right-end replication origin of parvoviruses minute virus of mice and LuIII. J. Virol 79, 2287–2300.

Cotmore, S.F., Tattersall, P., 2007. Parvoviral host range and cell entry mechanisms. Adv. Virus Res. *70*, 183–232.

Cotmore, S.F., Tattersall, P., 2013. Parvovirus diversity and DNA damage responses. In: Bell, S.D., Mechali, M., DePamphilis (Eds.), DNA Replication. Cold Spring Harbor Perspectives in Biology. Cold Spring Harbor Laboratory Press, pp. 457–468.

Cotmore, S.F., D'Abramo Jr., A.M., Carbonell, L.F., Bratton, J., Tattersall, P., 1997. The NS2 Polypeptide of parvovirus MVM is required for capsid assembly in murine cells. Virology *231*, 267–280.

Cotmore, S.F., Hafenstein, S., Tattersall, P., 2010. Depletion of virion-associated divalent cations induces parvovirus minute virus of mice to eject its genome in a 3"-to-5" direction from an otherwise intact viral particle. J. Virol. *84*, 1945–1956.

D'Abramo, A.M., Ali, A.A., Wang, F., Cotmore, S.F., Tattersall, P., 2005. Host range mutants of minute virus of mice with a single VP2 amino acid change require additional silent mutations that regulate NS2 accumulation. Virology *340*, 143–154.

Davies, H., Bignell, G.R., Cox, C., Stephens, P., Edkins, S., Clegg, S., Teague, J., Woffendin, H., Garnett, M.J., Bottomley, W., et al., 2002. Mutations of the BRAF gene in human cancer. Nature *417*, 949–954.

Di Piazza, M., Mader, C., Geletneky, K., Herrero, Y., Calle, M., Weber, E., Schlehofer, J., Deleu, L., Rommelaere, J., 2007. Cytosolic activation of cathepsins mediates parvovirus H-1-induced killing of cisplatin and TRAIL-resistant glioma cells. J. Virol. *81*, 4186–4198.

Donahue, J.M., Mullen, J.T., Tanabe, K.K., 2002. Viral oncolysis. Surg. Oncol. Clin. N. Am. *11*, 661–680.

Dupont, F., Avalosse, B., Karim, A., Mine, N., Bosseler, M., Maron, A., Van den Broeke, A.V., Ghanem, G.E., Burny, A., Zeicher, M., 2000. Tumor-selective gene transduction and cell killing with an oncotropic autonomous parvovirus-based vector. Gene Ther *7*, 790–796.

Dupont, F., 2003. Risk assessment of the use of autonomous parvovirus-based vectors. Curr Gene Ther *3*, 567–582.

Eichwald, V., Daeffler, L., Klein, M., Rommelaere, J., Salomé, N., 2002. The NS2 proteins of parvovirus minute virus of mice are required for efficient nuclear egress of progeny virions in mouse cells. J. Virol *76*, 10307–10319.

El Bakkouri, K., Servais, C., Clément, N., Cheong, S.C., Franssen, J.-D., Velu, T., Brandenburger, A., 2005. In vivo anti-tumour activity of recombinant MVM parvoviral vectors carrying the human interleukin-2 cDNA. J Gene Med *7*, 189–197.

Farr, G.A., Tattersall, P., 2004. A conserved leucine that constricts the pore through the capsid fivefold cylinder plays a central role in parvoviral infection. Virology *323*, 243–256.

Gardiner, E.M., Tattersall, P., 1988. Evidence that developmentally regulated control of gene expression by a parvoviral allotropic determinant is particle mediated. J. Virol *62*, 1713–1722.

Garraway, L.A., Widlund, H.R., Rubin, M.A., Getz, G., Berger, A.J., Ramaswamy, S., Beroukhim, R., Milner, D.A., Granter, S.R., Du, J., et al., 2005. Integrative genomic analyses identify MITF as a lineage survival oncogene amplified in malignant melanoma. Nature *436*, 117–122.

Geletneky, K., Kiprianova, I., Ayache, A., Koch, R., Herrero, Y., Calle, M., Deleu, L., Sommer, C., Thomas, N., Rommelaere, J., Schlehofer, J.R., 2010. Regression of advanced rat and human gliomas by local or systemic treatment with oncolytic parvovirus H-1 in rat models. Neuro-Oncology *12*, 804–814.

Grekova, S.P., Raykov, Z., Zawatzky, R., Rommelaere, J., Koch, U., 2012. Activation of a glioma-specific immune response by oncolytic parvovirus minute virus of mice infection. Cancer Gene Ther *19*, 468–475.

Grekova, S., Aprahamian, M., Giese, N., Schmitt, S., Giese, T., Falk, C.S., Daeffler, L., Czriepluch, C., Rommelaere, J., Raykov, Z., 2011. Immune cells participate in the oncosuppressive activity of parvovirus H-1PV and are activated as a result of their abortive infection with this agent. Cancer Biol. Ther. *10*, 1280–1289.

Gupta, P.B., Kuperwasser, C., Brunet, J.-P., Ramaswamy, S., Kuo, W.-L., Gray, J.W., Naber, S.P., Weinberg, R.A., 2005. The melanocyte differentiation program predisposes to metastasis after neoplastic transformation. Nat. Genet. *37*, 1047–1054.

Hallauer, C., Siegl, G., Kronauer, G., 1972. Parvoviruses as contaminants of permanent human cell lines. 3. Biological properties of the isolated viruses. Arch. Gesamte Virusforsch. *38*, 366–382.

Hocker, T.L., Singh, M.K., Tsao, H., 2008. Melanoma genetics and therapeutic approaches in the 21st century: moving from the benchside to the bedside. J. Invest. Dermatol. *128*, 2575–2595.

Lang, S.I., Giese, N.A., Rommelaere, J., Dinsart, C., Cornelis, J.J., 2006. Humoral immune responses against minute virus of mice vectors. J. Gene Med. *8*, 1141–1150.

Maroto, B., Valle, N., Saffrich, R., Almendral, J.M., 2004. Nuclear export of the nonenveloped parvovirus virion is directed by an unordered protein signal exposed on the capsid surface. J. Virol. *78*, 10685–10694.

Miller, C.L., Pintel, D.J., 2002. Interaction between parvovirus NS2 protein and nuclear export factor Crm1 is important for viral egress from the nucleus of murine cells. J. Virol. *76*, 3257–3266.

Mincberg, M., Gopas, J., Tal, J., 2011. Minute virus of mice (MVMp) infection and NS1 expression induce p53 independent apoptosis in transformed rat fibroblast cells. Virology *412*, 233–243.

Moehler, M., Blechacz, B., Weiskopf, N., Zeidler, M., Stremmel, W., Rommelaere, J., Galle, P.R., Cornelis, J.J., 2001. Effective infection, apoptotic cell killing and gene transfer of human hepatoma cells but not primary hepatocytes by parvovirus H1 and derived vectors. Cancer Gene Ther. *8*, 158–167.

Naeger, L.K., Cater, J., Pintel, D.J., 1990. The small nonstructural protein (NS2) of the parvovirus minute virus of mice is required for efficient DNA replication and infectious virus production in a cell-type-specific manner. J. Virol. *64*, 6166–6175.

Naeger, L.K., Salomé, N., Pintel, D.J., 1993. NS2 is required for efficient translation of viral mRNA in minute virus of mice-infected murine cells. J. Virol. *67*, 1034–1043.

Paglino, J., Burnett, E., Tattersall, P., 2007. Exploring the contribution of distal P4 promoter elements to the oncoselectivity of Minute Virus of Mice. Virology *361*, 174–184.

Paglino, J., Tattersall, P., 2011. The parvoviral capsid controls an intracellular phase of infection essential for efficient killing of stepwise-transformed human fibroblasts. Virology *416*, 32–41.

Paradiso, P.R., 1981. Infectious process of the parvovirus H-1: correlation of protein content, particle density, and viral infectivity. J. Virol. *39*, 800–807.

Parrish, C.R., Carmichael, L.E., 1986. Characterization and recombination mapping of an antigenic and host range mutation of canine parvovirus. Virology *148*, 121–132.

Prestwich, R.J., Harrington, K.J., Pandha, H.S., Vile, R.G., Melcher, A.A., Errington, F., 2008. Oncolytic viruses: a novel form of immunotherapy. Expert Rev. Anticancer Ther. *8*, 1581–1588.

Previsani, N., Fontana, S., Hirt, B., Beard, P., 1997. Growth of the parvovirus minute virus of mice MVMp3 in EL4 lymphocytes is restricted after cell entry and before viral DNA amplification: cell-specific differences in virus uncoating in vitro. J. Virol. *71*, 7769–7780.

Ran, Z., Rayet, B., Rommelaere, J., Faisst, S., 1999. Parvovirus H-1-induced cell death: influence of intracellular NAD consumption on the regulation of necrosis and apoptosis. Virus Res. *65*, 161–174.

Ravnan, M.C., Matalka, M.S., 2012. Vemurafenib in patients with BRAF V600E mutation-positive advanced melanoma. Clin. Ther. *34*, 1474–1486.

Rayet, B., Lopez-Guerrero, J.A., Rommelaere, J., Dinsart, C., 1998. Induction of programmed cell death by parvovirus H-1 in U937 cells: connection with the tumor necrosis factor alpha signalling pathway. J. Virol. *72*, 8893–8903.

Raykov, Z., Grekova, S., Galabov, A.S., Balboni, G., Koch, U., Aprahamian, M., Rommelaere, J., 2007. Combined oncolytic and vaccination activities of parvovirus H-1 in a metastatic tumor model. Oncol. Rep. *17*, 1493–1499.

Raykov, Z., Savelyeva, L., Balboni, G., Giese, T., Rommelaere, J., Giese, N.A., 2005. B1 lymphocytes and myeloid dendritic cells in lymphoid organs are preferential extratumoral sites of parvovirus minute virus of mice prototype strain expression. J. Virol. *79*, 3517–3524.

Robert, C., Thomas, L., Bondarenko, I., O'Day, S.M.D.J.W., Garbe, C., Lebbe, C., Baurain, J.-F., Testori, A., Grob, J.-J., et al., 2011. Ipilimumab plus dacarbazine for previously untreated metastatic melanoma. N. Engl. J. Med. *364*, 2517–2526.

Rubio, M.P., Guerra, S., Almendral, J.M., 2001. Genome replication and postencapsidation functions mapping to the nonstructural gene restrict the host range of a murine parvovirus in human cells. J. Virol. *75*, 11573–11582.

Ruiz, Z., Mihaylov, I.S., Cotmore, S.F., Tattersall, P., 2011. Recruitment of DNA replication and damage response proteins to viral replication centers during infection with NS2 mutants of minute virus of mice (MVM). Virology *410*, 375–384.

Tijssen, P., Agbandje-McKenna, M., Almendral, J.M., Bergoin, M., Flegel, T.W., Hedman, K., Kleinschmidt, J.A., Li, Y., Pintel, D.J., Tattersall., P., 2011. Parvoviridae. In: King, A.M.Q., Adams, M.J., Carstens, E., Lefkowitz, E.J. (Eds.), Virus Taxonomy: Classification and Nomenclature of Viruses: Ninth Report of the International Committee on Taxonomy of Viruses. Elsevier, San Diego, pp. 375–395.

Tworkoski, K., Singhal, G., Szpakowski, S., Zito, C.I., Bacchiocchi, A., Muthusamy, V., Bosenberg, M., Krauthammer, M., Halaban, R., Stern, D.F., 2011. Phosphoproteomic screen identifies potential therapeutic targets in melanoma. Mol. Cancer Res. *9*, 801–812.

Wetzel, K., Struyf, S., Van Damme, J., Kayser, T., Vecchi, A., Sozzani, S., Rommelaere, J., Cornelis, J.J., Dinsart, C., 2007. MCP-3 (CCL7) delivered by parvovirus MVMp reduces tumorigenicity of mouse melanoma cells through activation of T lymphocytes and NK cells. Int. J. Cancer *120*, 1364–1371.

Wolchok, J., 2012. How recent advances in immunotherapy are changing the standard of care for patients with metastatic melanoma. Ann. Oncol. (*Suppl 8*), viii15–viii2123 (*Suppl 8*), viii15–viii21.

Wollmann, G., Ozduman, K., van den Pol, A.N., 2012. Oncolytic virus therapy for glioblastoma multiforme. Cancer J. *18*, 69–81.

Yeung, D.E., Brown, G.W., Tam, P., Russnak, R.H., Wilson, G., Clark-Lewis, I., Astell, C. R., 1991. Monoclonal antibodies to the major nonstructural nuclear protein of minute virus of mice. Virology *181*, 35–45.

Zitvogel, L., Apetoh, L., Ghiringhelli, F., André, F., Tesniere, A., Kroemer, G., 2008. The anticancer immune response: indispensable for therapeutic success? J. Clin. Invest. *118*, 1991–2001.